J Biol Inorg Chem
DOI 10.1007/s00775-014-1124-7

ORIGINAL PAPER

Pseudoazurin from *Sinorhizobium meliloti* as an electron donor to copper-containing nitrite reductase: influence of the redox partner on the reduction potentials of the enzyme copper centers

Félix M. Ferroni · Jacopo Marangon · Nicolás I. Neuman · Julio C. Cristaldi · Silvina M. Brambilla · Sergio A. Guerrero · María G. Rivas · Alberto C. Rizzi · Carlos D. Brondino

Received: 8 October 2013 / Accepted: 10 March 2014

Abstract Pseudoazurin (Paz) is the physiological electron donor to copper-containing nitrite reductase (Nir), which catalyzes the reduction of NO_2^- to NO. The Nir reaction mechanism involves the reduction of the type 1 (T1) copper electron transfer center by the external physiological electron donor, intramolecular electron transfer from the T1 copper center to the T2 copper center, and nitrite reduction at the type 2 (T2) copper catalytic center. We report the cloning, expression, and characterization of Paz from *Sinorhizobium meliloti* 2011 (SmPaz), the ability of SmPaz to act as an electron donor partner of *S. meliloti* 2011 Nir (SmNir), and the redox properties of the metal centers involved in the electron transfer chain. Gel filtration chromatography and sodium dodecyl sulfate–polyacrylamide gel electrophoresis together with UV–vis and EPR spectroscopies revealed that as-purified SmPaz is a mononuclear copper-containing protein that has a T1 copper site in a highly distorted tetrahedral geometry. The SmPaz/SmNir interaction investigated electrochemically showed that SmPaz serves as an efficient electron donor to SmNir. The formal reduction potentials of the T1 copper center in SmPaz and the T1 and T2 copper centers in SmNir, evaluated by cyclic voltammetry and by UV-vis- and EPR-mediated potentiometric titrations, are against an efficient Paz T1 center to Nir T1 center to Nir T2 center electron transfer. EPR experiments proved that as a result of the SmPaz/SmNir interaction in the presence of nitrite, the order of the reduction potentials of SmNir reversed, in line with T1 center to T2 center electron transfer being thermodynamically more favorable.

Keywords Pseudoazurin · Nitrite reductase · Electrochemistry · Redox titration · EPR

Electronic supplementary material The online version of this article (doi:10.1007/s00775-014-1124-7) contains supplementary material, which is available to authorized users.

F. M. Ferroni · N. I. Neuman · J. C. Cristaldi · S. M. Brambilla · M. G. Rivas · A. C. Rizzi · C. D. Brondino (✉)
Departamento de Física, Facultad de Bioquímica y Ciencias Biológicas, Universidad Nacional del Litoral, Ciudad Universitaria, Paraje El Pozo, S3000ZAA Santa Fe, Argentina
e-mail: brondino@fbcb.unl.edu.ar

J. Marangon · M. G. Rivas
REQUIMTE/CQFB, Departamento de Quimica, Faculdade de Ciências e Tecnologia, Universidade Nova de Lisboa, 2829-516 Caparica, Portugal

S. A. Guerrero
Laboratorio de Bioquímica Microbiana, Instituto de Agrobiotecnología del Litoral, Universidad Nacional del Litoral, Ciudad Universitaria, Paraje El Pozo, S3000ZAA Santa Fe, Argentina

Introduction

The biogeochemical nitrogen cycle performed by bacteria involves important redox processes that include dinitrogen fixation, ammonification, nitrification, and denitrification [1–3]. Distinct types of microorganisms have been shown to have the machinery to perform these processes. Some of them, as is the case of rhizobia, live symbiotically in root nodules of legumes and are widely used in agriculture as fertilizers because of their ability to take dinitrogen from the atmosphere [4]. These organisms may also produce negative impacts in the environment because they can produce the greenhouse gas N_2O and acidification of soils [5–7].

Published online: 20 March 2014

Denitrification is the dissimilatory reduction of nitrate to dinitrogen. Nitrite reductase (Nir) is the enzyme that catalyzes the second step of this process through the one-electron reduction of NO_2^- to NO ($E^{o\prime} = 370$ mV). In the denitrifying bacterium *Sinorhizobium meliloti* this reaction is catalyzed by a green copper-containing Nir (SmNir) coded by the structural gene *nirK* [8–11]. SmNir, like most copper-containing Nir enzymes reported so far [12–14], has a homotrimeric structure with two copper atoms per monomer, one of type 1 (T1; also blue copper) and the other of type 2 (T2; also normal copper). The T1 and T2 copper centers, which are the electron transfer and the catalytic centers, respectively, are approximately 12 Å apart and are bridged by a histidine–cysteine pathway likely involved in electron transfer [15, 16]. The proposed reaction mechanism implies that nitrite binds to the T2 center and is converted to NO by reducing equivalents delivered by an external physiological electron donor through the T1 center [17].

The physiological electron donors of green Nir enzymes are small mononuclear copper proteins (approximately 13 kDa) called pseudoazurins (Pazs) that belong to the cupredoxin family of proteins [18, 19]. Paz harbors a T1 copper site in a distorted tetrahedral geometry that comprises the thiolate sulfur atom of a cysteine residue, two imidazole nitrogen atoms of two histidine residues, and a weak bond with the sulfur atom of a methionine residue [20–25]. Paz interacts with structurally different redox partners, an ability that seems to be associated with the hydrophobic character of the binding surface centered at the electron entry/exit point [26]. Other factors such as the presence of charged side chains and the molecular dipole moment have also been suggested to play a role in the orientation of the two redox partners prior to collision [27].

The study of the catalytic mechanism of Nir entails the investigation of three redox processes, the reduction of the T1 copper center by the external physiological electron donor, intramolecular electron transfer from the T1 copper center to the T2 copper center, and nitrite reduction at the T2 copper center. We have recently reported the molecular, kinetic, and spectroscopic properties of a recombinant Nir (locus tag SMa1250) from *S. meliloti* 2011 using an artificial electron donor [11]. The genome sequence of this bacterium codes for several putative nitrogen-metabolism-related proteins. A 53-kb segment of pSymA megaplasmid is particularly rich in such genes, including a complete pathway for denitrification that surrounds the nitrogen fixation gene cluster [8, 28]. Two genes coding for Pazs are present: one of them is located in the pSymA megaplasmid (*azu1*, locus tag SMa1243), and the other is situated in the genophore (*azu2*, locus tag SMc04047). The product of *azu2* is a small blue cupredoxin involved in sulfur metabolism that acts as an electron donor for SorT sulfite dehydrogenase [29, 30]. The product of *azu1*, hereafter SmPaz, is directly related to the denitrification segment of pSymA, and has not been investigated yet as a physiological electron donor to SmNir.

In this work we report the cloning, expression, and characterization of SmPaz and its ability to act as an electron donor to SmNir. The SmPaz/SmNir interaction is investigated electrochemically. To characterize the electron transfer chain involved in nitrite reduction, the formal reduction potentials of the T1 copper center in SmPaz and the T1 and T2 copper centers in SmNir were evaluated by cyclic voltammetry and by UV–vis- and EPR-mediated potentiometric titrations. We analyze the role of SmPaz in modulating the reduction potentials of the copper centers in SmNir leading to a thermodynamically favorable electron transfer process.

Materials and methods

Sinorhizobium meliloti 2011 growth conditions, DNA extraction, and cloning of *azu1*

The growth of *S. meliloti* 2011 cells and DNA extraction were performed as reported elsewhere [11]. The *S. meliloti azu1* gene (locus tag SMa1243) was amplified using two specific oligonucleotides (5′-CATATGCGCATAATCGC AAAG-3′ and 5′-GAGCTCCTATTGGAGGGCCAC-3′, forward and reverse, respectively) which include the *Nde*I and *Sac*I restriction sites. Amplification was performed using *Pfu* DNA polymerase from Genbiotech according to the manufacturer's instructions. The *azu1* gene was cloned into the *Fau*NDI/*Sac*I-digested pET22b(+) vector (Novagen) to obtain p22SPaz expression constructs. The p22SPaz plasmids were used to transform *Escherichia coli* BL21 (DE3) cells.

Overexpression and purification

Escherichia coli BL21 (DE3) cells containing p22SPaz were aerobically cultured at 30 °C and 200 rpm in lysogeny broth supplemented with 0.6 mM $CuSO_4$. Protein expression was induced at $A_{600\ nm} \sim 0.6$ using 0.25 mM isopropyl β-D-thiogalactopyranoside for 3 h. Following cell harvest and suspension in 20 mM tris(hydroxymethyl)aminomethane (Tris)–HCl buffer pH 6.0, cells were disrupted by sonication. The crude extract was centrifuged (25,000*g* for 1 h), and the supernatant was dialyzed for 4 h against 20 mM Tris–HCl buffer pH 6.0 supplemented with 0.6 mM $CuSO_4$. The soluble fraction was submitted to a two-step purification process which includes a Source 15Q matrix column (1.6 cm × 13 cm, GE Pharmacia Biotech, equilibrated with 20 mM Tris–HCl pH 6.0 plus 50 mM

NaCl) and a Superdex 200 matrix column (1.5 cm × 42 cm, GE Healthcare, equilibrated with 200 mM NaCl/20 mM Tris–HCl pH 7.0). After the second purification step, the fractions containing pure SmPaz were collected, concentrated, and kept at −80 °C until use.

Overexpression and purification of SmNir were performed as reported previously [11].

Protein quantification, molecular mass determination, and metal analysis

The protein concentration was determined using the Bradford method with bovine serum albumin as a standard [31]. The molecular mass of the as-isolated enzyme was estimated by gel filtration chromatography using a prepacked Superdex 200 HR 10/30 column (GE Healthcare) equilibrated with 50 mM potassium phosphate buffer and 150 mM NaCl pH 7.6 connected to a high-performance liquid chromatography device (ÄKTAbasic, GE Healthcare). The molecular mass markers (GE Healthcare) used for calibration were ferritin (440 kDa), conalbumin (75 kDa), carbonic anhydrase (29 kDa), and ribonuclease A (13.7 kDa).

Sodium dodecyl sulfate–polyacrylamide gel electrophoresis (15 %) under reducing conditions was performed according to the method of Laemmli [32]. The molecular mass markers (GE Healthcare) for calibration were phosphorylase b (97.0 kDa), albumin (66.0 kDa), ovalbumin (45.0 kDa), carbonic anhydrase (30.0 kDa), trypsin inhibitor (20.1 kDa), and α-lactalbumin (14.4 kDa).

The copper content of SmPaz was determined by atomic absorption spectrometry using a PerkinElmer Analyst 800 spectrometer.

Spectroscopic methods

UV–vis spectra were recorded with a PerkinElmer Lambda 20 UV–vis spectrophotometer. EPR measurements were performed at X-band with a Bruker EMX Plus spectrometer equipped with a universal high-sensitivity cavity (HSW10819 model) and with an Oxford Instruments helium continuous-flow cryostat. Spectra were acquired under nonsaturating conditions. The experimental conditions were as follows: microwave frequency, 9.45 GHz; modulation field, 100 kHz; modulation amplitude, 2 G; microwave power, 0.2 mW; temperature, −213 °C. EPR spectra were simulated with the EasySpin toolbox for MATLAB® [33].

EPR- and UV–vis-mediated redox titrations

EPR redox titration was performed as reported elsewhere [34] with some modifications. The SmNir sample (approximately 200 μM protein in 150 mM Tris–HCl pH 7) was placed in a vessel under anaerobic conditions provided by a Schlenk-type line. Protein samples (200 μL) were withdrawn by a gastight syringe from the vessel after at least 15 min had been allowed for redox equilibrium to be achieved, loaded into argon-flushed EPR tubes, and frozen under liquid nitrogen until use.

UV–vis redox titration of SmNir (approximately 200 μM protein in 150 mM Tris–HCl pH 7) was performed under anaerobic conditions at room temperature as described elsewhere [35], following the reaction at 586 nm. Dithionite and ferricyanide were the reductant and the oxidant, respectively, for both titrations. The potentials were measured using platinum and Ag/AgCl/KCl (3 M) electrodes calibrated with saturated quinhydrone solution at pH 7.0 and pH 4.0 at room temperature. All the potentials are referred to the standard hydrogen electrode (SHE).

Electrochemistry

Cyclic voltammetry experiments were performed with an AUTOLAB type III potentiostat/galvanostat from ECO Chemie (Utrecht, The Netherlands). The data were collected and analyzed using the GPES software package from ECO Chemie. A conventional three-electrode configuration glass cell composed of a platinum wire counter electrode and a saturated Ag/AgCl reference electrode (197 mV vs SHE at room temperature) was used. The working electrode was a gold disk electrode with a nominal radius of 0.8 mm and an effective surface area of 0.0195 cm^2. The gold electrode was polished with 0.05-μm water alumina slurry (Buehler) and then sonicated in water. The polished electrode was subsequently immersed in 1 mM 4,4′-dithiodipyridine solution for a few minutes; 4,4′-dithiodipyridine acts as a promoter of the enzyme–electrode interaction (see Scheme S1) [36]. Then, 2 μL of 250 μM SmPaz solution in 50 mM phosphate buffer pH 7 was deposited on the polished electrode, and a square piece of the negatively charged dialysis membrane (3,500-Da cutoff) was placed on the top of the electrode. Finally, a rubber ring was fitted around the electrode body, entrapping the enzyme solution at the electrode–membrane interface, forming a uniform thin layer. The membrane electrode was then placed in the electrolytic solution. This electrode configuration allows small ions to diffuse throughout the membrane, keeping at the same time the protein trapped close to the electrode [37]. The potential was cycled at different scan rates (5 mV $s^{-1} < v < 100$ mV s^{-1}). Both 50 mM phosphate buffer pH 7 and 50 mM buffer mixture [2-(*N*-morpholino)ethanesulfonic acid, *N*-(2-hydroxyethyl)piperazine-*N*′-ethanesulfonic acid, *N*-cyclohexyl-3-aminopropanesulfonic acid, *N*-[tris(hydroxymethyl)methyl]-3-aminopropanesulfonic acid], $5 < pH < 10$, were used as electrolytes. The solutions were degassed, and the experiment was

conducted under an argon atmosphere. The measurements were performed at room temperature.

All the reagents and buffer electrolytes were of analytical grade (Sigma) and were prepared using Milli-Q water with a resistivity of 18 MΩ cm. All the potentials are referred to the SHE.

SmNir activity assay using SmPaz as an electron donor

SmPaz/SmNir interaction was also evaluated with a continuous spectrophotometric assay following oxidation of reduced SmPaz in the presence of SmNir and nitrite. A solution containing an SmNir-to-SmPaz ratio of 1:100 was agron-fluxed for 15 min in a sealed 1 cm path length UV–vis cell under continuous stirring. This solution was reduced by adding by means of a gastight Hamilton syringe the necessary amount of a freshly prepared argon-degassed sodium dithionite solution (50 mM) under anaerobic conditions to reduce the enzymes completely. The enzyme reduction was considered to be complete when no SmPaz absorption band at 597 nm was observed. The reaction was started by adding 45 µL of an argon-degassed 150 mM sodium nitrite solution. All the solutions were prepared in 100 mM Tris–HCl pH 7.0. The final concentrations were 60 nM SmNir, 6 µM SmPaz, and 2.5 mM nitrite, and the final volume was 2.7 mL. The oxidation of reduced SmPaz was followed by UV–vis spectroscopy.

Results and discussion

Molecular properties, UV–vis spectra, and EPR spectra of SmPaz

The *azu1* gene coding for a putative Paz was cloned and overexpressed in *E. coli* BL21 (DE3) cells and purified to electrophoretic grade as explained in "Overexpression and purification," with a yield of 72 mg protein per liter of culture.

Alignment of the amino acid sequence of SmPaz and the amino acid sequences of Paz from other bacteria is shown in Fig. S1. SmPaz exhibits 65.8 % sequence identity with Paz from *Achromobacter cycloclastes*, 57.1 % sequence identity with Paz from *Alcaligenes faecalis* S-6 and *Paracoccus pantotrophus*, 47.7 % sequence identity with Paz from *Methylobacterium extorquens* AM1, 44.7 % sequence identity with *azu2* from *S. meliloti*, and 38.4 % sequence identity with Paz from *Hyphomicrobium denitrificans*.

Molecular mass determination by gel filtration of SmPaz from the soluble fraction yielded a value of approximately 16 kDa, whereas sodium dodecyl sulfate–polyacrylamide gel electrophoresis showed a unique band with a molecular mass of approximately 13 kDa (Fig. 1, upper panel, inset),

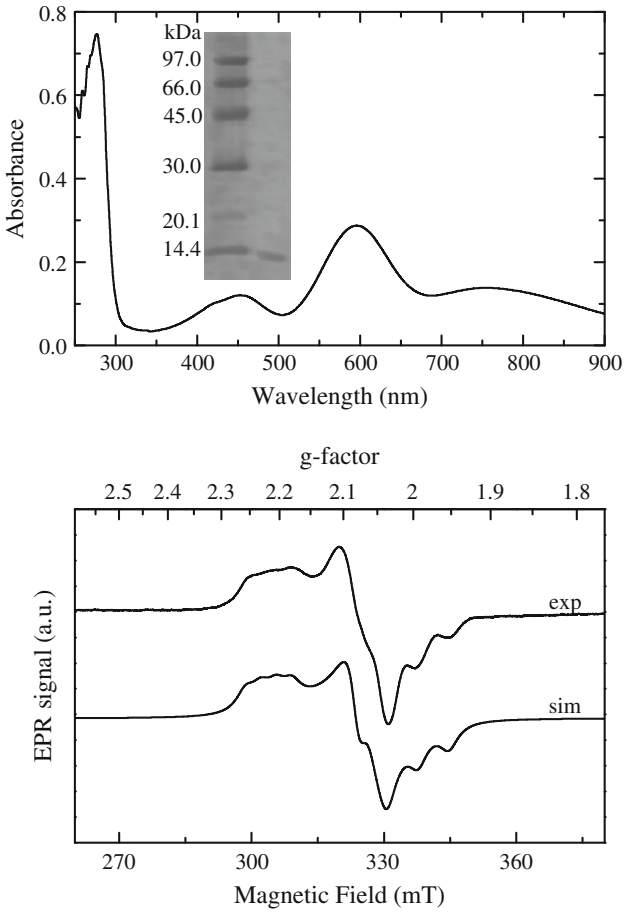

Fig. 1 *Top*: Electronic absorption spectrum of pseudoazurin from *Sinorhizobium meliloti* 2011 (SmPaz). The *inset* shows the sodium dodecyl sulfate–polyacrylamide gel electrophoresis of SmPaz. *Bottom* X-band EPR spectrum (*exp*) of SmPaz together with the simulated spectrum (*sim*). *g* and *A* values are indicated in the text. The linewidth used in the simulation was 3 mT

indicating that as-purified SmPaz is a monomer. Most Pazs as well as azurins isolated from different sources were found to be a monomer in both the oxidized and the reduced forms [20, 24, 38], with the only exception being dimeric *P. pantotrophus* Paz [27]. Metal analysis identified 0.8 ± 0.1 copper atoms per protein, in agreement with values reported in the literature [20, 21, 23, 38].

The UV–vis spectrum (Fig. 1, upper panel) of as-purified SmPaz is typical of distorted T1 copper sites and shows principal absorption maxima at 597 nm ($\varepsilon = 3.17 \pm 0.03$ mM^{-1} cm^{-1}) and 460 nm ($\varepsilon = 1.5 \pm 0.1$ mM^{-1} cm^{-1}), corresponding to S-Cys $\sigma \rightarrow$ Cu $d_{x^2-y^2}$ and S-Cys $\pi \rightarrow$ Cu $d_{x^2-y^2}$ charge transfer bands, respectively [39]. Similar spectra were observed for Paz from other sources [40, 41]. The addition of either sodium ascorbate or sodium dithionite led to the disappearance of all visible bands (not shown), consistent with a T1 center in its reduced form.

The EPR spectrum of SmPaz obtained at X-band is presented in the lower panel in Fig. 1, together with the simulated spectrum. The as-purified SmPaz spectrum exhibits rhombic symmetry ($g_1 = 2.221$, $g_2 = 2.060$, $g_3 = 2.019$, $A_1 = 3.5$ mT, $A_2 = 0.9$ mT, $A_3 = 6.9$ mT). No hyperfine structure attributable to nitrogen nuclei from the two histidine residues coordinated to the copper atom was detected. Addition of ascorbate or dithionite to SmPaz under anaerobic conditions reduces completely the copper center, which becomes EPR-silent (not shown). The EPR spectrum of SmPaz departs considerably from the axial spectrum observed in classic blue copper proteins ($g_{\|} \sim 2.22$, $A_{\|} \sim 6$ mT, no solved hyperfine structure at $g_{\perp}$). This fact, together with the enhanced 460-nm UV–vis absorption band (see Fig. 1, upper panel), indicates a T1 copper site in a highly distorted tetrahedral geometry [39].

Electrochemistry of SmPaz

Direct electrochemistry of SmPaz was performed on a gold membrane electrode as described in "Electrochemistry." The cyclic voltammograms show a reversible response characterized by reductive (E_{pc}) and oxidative (E_{pa}) peaks (Fig. 2, upper panel). Two different behaviors describe the peak current variation with the scan rate. For low scan rates (5 mV $s^{-1} < v < 50$ mV s^{-1}), the intensity of the peak (i_p) varies linearly with the scan rate (Fig. S2, upper panel), indicating a thin-layer regime. For high scan rates ($v > 50$ mV s^{-1}), the intensity of the peak varies linearly with the square root of the scan rate (Fig. S2, lower panel), typical of a diffusion-controlled regime. The half-height width was about 90 mV for both cathodic and anodic peaks over all the scan rate range tested, indicating a reversible one-electron process [42]. The formal reduction potential, which corresponds to the average between the cathodic and anodic peaks, $E^{o\prime} = (E_{pc} + E_{pa})/2$, was determined to be $E^{o\prime} = 278 \pm 6$ mV vs SHE (the E_{pc} and E_{pa} values as a function of the scan rate are shown in Fig. S3). This reduction potential is in line with the potentials determined for Paz from *A. faecalis*, 270 mV [40], *A. cycloclastes*, 260 mV [41], and *P. pantotrophus*, 230 mV [43].

SmPaz as an electron donor to SmNir assessed by electrochemistry

To test the ability of SmPaz to act as electron donor to SmNir, both proteins were confined on a gold membrane electrode in the presence of 1 mM $NaNO_2$ and different Nir-to-Paz ratios (Fig. 2, lower panel). SmPaz in the absence of SmNir (Fig. 2, lower panel, voltammogram a) showed behavior similar to that shown in the upper panel in Fig. 2, whereas SmNir alone did not exhibit any catalytic response (not shown). In the presence of SmNir,

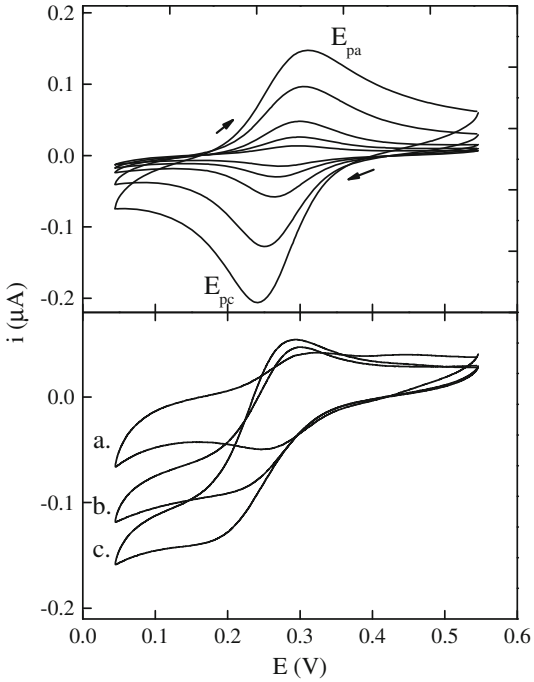

Fig. 2 *Top*: Cyclic voltammograms of SmPaz for different scan rates (5 mV $s^{-1} < v < 100$ mV s^{-1}) (E_{pc} cathodic peak potential, E_{pa} anodic peak potential). *Bottom*: Representative cyclic voltammograms ($v = 20$ mV s^{-1}) of 250 μM SmPaz in the presence of 1 mM $NaNO_2$ and increasing concentrations of *S. meliloti* 2011 nitrite reductase (SmNir)— without SmNir (*a*), with 25 μM SmNir (*b*), and with 50 μM SmNir (*c*)

the cyclic voltammograms exhibit a sigmoidal shape with enhanced cathodic currents. The higher the SmNir concentration, the higher the cathodic signal, which confirms that SmNir is the catalytic component, whereas SmPaz mediates the electron transfer between SmNir and the electrode.

The kinetic properties of the SmNir/SmPaz couple were evaluated by varying the nitrite concentration using an SmPaz-to-SmNir ratio of approximately 1:1. The increase of substrate concentration causes an increase of the catalytic current until saturation (Figs. S4, S5), indicating that the catalytic current resembles the rate of catalysis predicted by a Michaelis–Menten model. A least-squares fitting of the catalytic current as a function of the nitrite concentration using this model (Fig. 3) allowed us to obtain an apparent Michaelis constant, K_m^{app}, of 100 ± 8 μM. This value is lower than that reported previously for SmNir ($K_m = 550 \pm 60$ μM) when methyl viologen was used as an electron donor [11]. The significant decrease in K_m when using SmPaz as the redox partner, together with the fact that the genes coding for both proteins are simultaneously expressed under denitrifying conditions [28], strongly suggests that SmPaz is the physiological electron donor to SmNir.

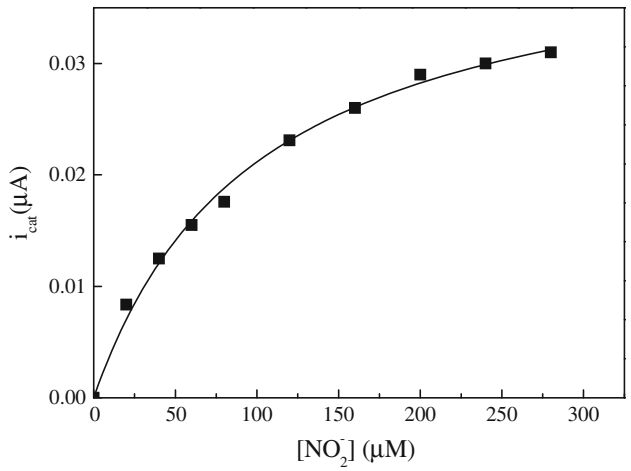

Fig. 3 Variation of the catalytic current with the nitrite concentration (10 μM < NO_2^- < 280 μM). The *solid line* is a least-squares fitting with the Michaelis–Menten model

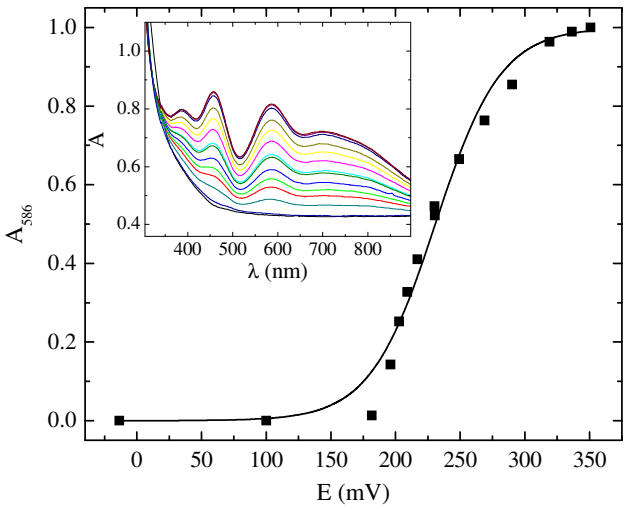

Fig. 4 Redox potentiometric titration of the type 1 center in SmNir monitored by UV–vis spectroscopy. The UV–vis spectra as a function of the potential are shown in the *inset*

Reduction potentials of SmNir determined by UV–vis- and EPR-mediated redox titrations

Understanding at the molecular level of the SmNir catalytic mechanism and its relationship with the intramolecular electron transfer process requires the determination of the reduction potentials of the T1 and T2 centers. As they could not be determined by cyclic voltammetry (see earlier), we performed UV–vis- and EPR-mediated redox titrations. The former was used to determine the reduction potential of the T1 center by monitoring the changes in the intensity of the UV–vis absorption band at 586 nm, whereas the latter was used to determine the reduction potentials of the T1 and T2 centers by monitoring the EPR signal intensity associated with each center.

Figures 4 and 5 show the redox potentiometric titration curves of SmNir monitored by UV–vis spectroscopy and EPR spectroscopy, respectively. The UV–vis spectra at different potentials are shown in the inset in Fig. 4. Least-squares fitting with the Nernst equation to the data yielded $E^{o\prime} = 226 \pm 3$ mV with $n = 1.0 \pm 0.1$ for the reduction potential of the T1 center. The EPR spectra at different potentials are shown in the inset in Fig. 5. As previously reported, the EPR spectrum of as-purified SmNir exhibits two magnetically different components in a 1:1 ratio associated with the T1 and T2 centers ($g_1 = 2.190$, $g_2 = 2.062$, $g_3 = 2.033$, $A_1 = 5.8$ mT for the T1 center; $g_{\|} = 2.304$, $g_{\perp} = 2.053$, $A_{\|} = 14$ mT for the T2 center) [11]. It is important to note that the EPR $g_{\|}$ features of the T2 center show some changes in lineshape together with a shifting to higher magnetic field on reduction (see the inset in Fig. 5). These spectral modifications may be attributed to possible structural changes of the T2 site on reduction

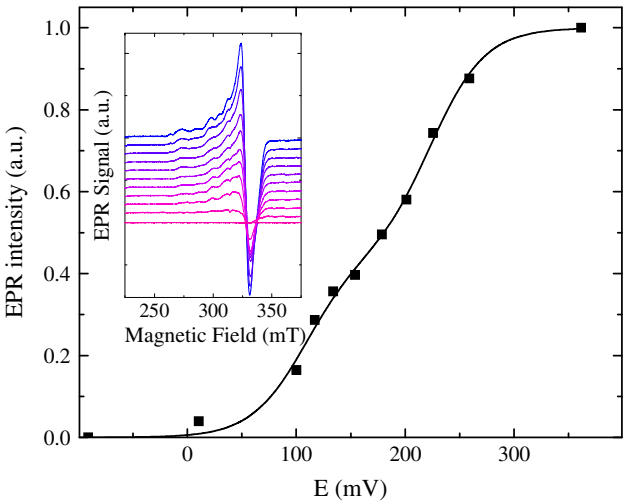

Fig. 5 Redox potentiometric titration of SmNir monitored by EPR spectroscopy. The *solid line* was obtained by least squares fitting a two-independent-component Nernst equation with $n = 1$ to the data. The EPR spectra as a function of the potential are shown in the *inset*

and/or exchange interactions between the T1 and T2 centers mediated by the histidine–cysteine pathway proposed to be involved in electron transfer during catalysis.

Different strategies were tested to evaluate the signal intensity associated with each spectral component. First, we tried to simulate the two-component spectrum, but the lineshape of the overall spectrum could not be reproduced well because of the spectral changes discussed above that were observed on reduction, which precluded the application of this method. A second approach was to evaluate the intensity of the nonoverlapping T2 center $g_{\|}$ feature.

However, this procedure had two limitations: the poor intensity-to-noise ratio of the peaks, and it solely evaluated the T2 center intensity. As we verified that the position of $g_\perp$ for both centers did not shift during the redox titration, we used a third strategy consisting in evaluating the intensity of the more intense spectral peak originating from the sum of the $g_\perp$ features of both T1 and T2 centers. The data obtained with this procedure are shown in Fig. 5, and were least squared fitted to a Nernst equation with two independent components, yielding $E^{o\prime} = 224 \pm 4$ mV for the T1 center and $E^{o\prime} = 108 \pm 5$ mV for the T2 center, values in line with those predicted from the behavior observed on enzyme reduction with ascorbate and dithionite [11] and with those obtained for other copper-containing Nir enzymes [17]. $E^{o\prime}$ of the T1 center obtained by EPR spectroscopy is in good agreement with that obtained by UV–vis spectroscopy.

SmNir reduction potential modulation by SmPaz

We performed EPR studies on a solution containing both proteins to evaluate possible changes in the EPR signal of SmNir in the presence of SmPaz under different experimental conditions. Spectrum a in Fig 6 is the spectrum of a mixture of SmNir and SmPaz under aerobic conditions showing the SmNir T1 center and T2 center signals in a 1:1 ratio. The T1 center signal of SmPaz (Fig. 1, lower panel) is not discernible because the mixture was prepared in an approximately 1:6 SmPaz-to-SmNir ratio. Reduction with excess dithionite of the SmNir/SmPaz mixture under anaerobic conditions produced an EPR-silent form (Fig. 6, spectrum b). Spectrum d in Fig. 6d is the spectrum of the dithionite-reduced SmNir/SmPaz mixture on reaction with the substrate nitrite, whereas spectrum c corresponds to the same experiment but performed in the absence of SmPaz. Although spectrum c shows that the T2 center intensity is greater than that of the T1 center, in line with the reduction potentials determined for both centers, spectrum d shows the opposite. As a control, the sample corresponding to spectrum d was reoxidized with ferricyanide under anaerobic conditions. This resulted in a spectrum similar to spectrum a in Fig. 6 (T1 center to T2 center EPR signal intensity ratio of approximately 1), which confirmed the integrity of the protein copper centers during the enzyme redox cycling and the shift of the reduction potentials.

In contrast to any unspecific oxidant, nitrite is the natural substrate of Nir, indicating that its oxidizing effect must necessarily be accomplished through an interaction between nitrite and the active site. A comparison of spectra c and d in Fig. 6 shows clearly that the interaction of SmPaz and SmNir on addition of nitrite changes the relative values of the T1 center and T2 center reduction potentials in SmNir, i.e., $E^{o\prime}_{T1} < E^{o\prime}_{T2}$, as the intensity of the

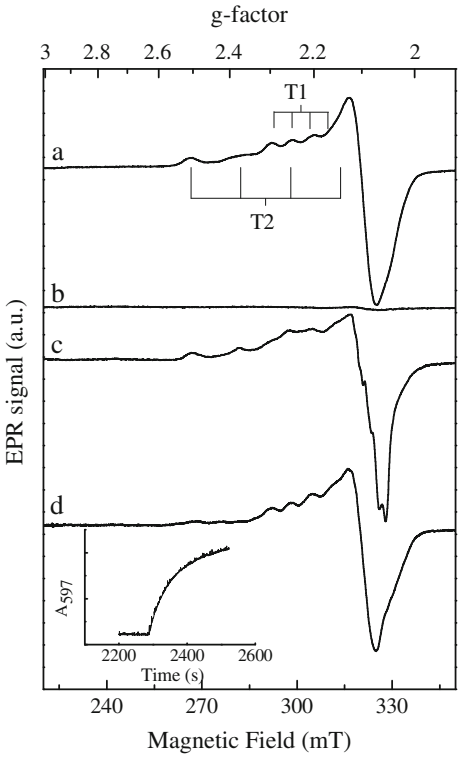

Fig. 6 EPR spectra of an SmNir/SmPaz mixture (*a*), a dithionite-reduced SmNir/SmPaz mixture (*b*), nitrite-reacted SmNir (*c*), and a nitrite-reacted SmNir/SmPaz mixture (*d*). The nitrite-reacted forms were obtained on incubation with the substrate for approximately 10 min under anaerobic conditions. The protein concentrations were approximately 200 μM for SmNir and approximately 35 μM for SmPaz in 100 mM tri(hydroxymethyl)aminomethane–HCl buffer pH 7.1. The final dithionite and nitrite concentrations were each 2 mM. The four hyperfine components at $g_\parallel$ of the type 1 and type 2 centers are indicated The. The *inset* shows the time variation of the absorbance at 597 nm of dithionite-reduced SmPaz in a solution containing SmNir and SmPaz in a ratio of 1:100. The absorbance increase is produced on addition of nitrite (see "SmNir activity assay using SmPaz as an electron donor" for details)

T1 center EPR signal is greater than that of the T2 center. This result, which to our knowledge has been observed for the first time in a copper-containing Nir, might indicate that the shift of the reduction potentials in SmNir is a consequence of the SmPaz/SmNir interaction.

The ability of SmPaz to serve as an electron donor to SmNir was tested as described in "SmNir activity assay using SmPaz as an electron donor." The inset in Fig. 6 shows that dithionite-reduced SmPaz in the presence of SmNir is oxidized on addition of nitrite, confirming that the EPR spectral changes (Fig. 6, spectrum d) experienced by SmNir are produced once the redox reaction between SmNir and SmPaz in the presence of the substrate has gone to completion. An additional redox titration using a mixture SmPaz and SmNir in a ratio of approximately 1:6 was performed in the absence of the substrate to test the influence of SmPaz alone on the reduction potentials of

SmNir (not shown). This experiment yielded reduction potentials, within experimental error, similar to those obtained for SmNir without SmPaz, confirming that the shifting of the reduction potentials is a consequence of the SmNir/SmPaz interaction in the presence of nitrite. Although the shifting of the reduction potentials is detected at the end of the reaction of SmNir with the physiological electron donor, it might also be operative during the reaction.

The T1 center reduction potentials of both SmPaz and SmNir and the T2 center reduction potential of as-purified SmNir are in line with those reported for Paz and Nir from other sources [40, 41, 44–47]. In principle, they do not favor an efficient Paz T1 center ($E^{o\prime} = 278$ mV) to Nir T1 center ($E^{o\prime} = 224$ mV) to Nir T2 center ($E^{o\prime} = 108$ mV) electron transfer, as the potential gradient does not favor the electron flow for nitrite reduction ($E^{o\prime} = 370$ mV). Experimental evidence from *Rhodobacter sphaeroides* Nir [46] and *Pseudomonas chlororaphis* Nir [45] suggested that nitrite/Nir interaction can reverse the order of the reduction potentials, which would favor the internal electron transfer. This is not the case in as-purified SmNir, as reoxidation with nitrite of the dithionite-reduced enzyme did not produce such an effect (Fig. 6, spectrum c) [11]. On the other hand, Prudêncio et al. [48] suggested that a favorable potential gradient could be produced on interaction of the enzyme with the physiological electron donor partner. Our findings are in line with their suggestion, since, as evidenced by our EPR results (Fig. 6, spectrum d), the interaction of SmNir with both SmPaz and nitrite inverts the order of the reduction potentials determined for as-purified SmNir once the reaction has gone to completion. This suggests that the T1 center to T2 center electron transfer is thermodynamically more favorable in the presence of both the physiological electron donor and the substrate.

Conclusions

The *azu1* gene in the *S. meliloti* genome codes for a Paz that serves as an efficient electron donor to the copper-containing SmNir. Although only a few works have been devoted to fully characterizing the reduction potentials of copper-containing Nir enzymes, the results obtained so far indicate that the Paz T1 center to Nir T1 center to Nir T2 center electron transfer is against the potential gradient. We have shown for the first time that the Nir/Paz interaction in the presence of nitrite changes the order of the reduction potentials determined for as-purified SmNir, which would favor the internal electron transfer. This evidence, together with what was found previously for the closely related *P. chlororaphis* Nir, indicates that copper-containing Nir enzymes may alternatively modulate the reduction potentials of the metal centers through interaction either with the substrate or with the physiological electron donor.

Acknowledgments The *S. meliloti* 2011 strain was kindly provided by A. Lagares (Universidad Nacional del Litoral). This work supported by projects PICT 2011-1654, CONICET PIP 112-2000801-01079, and CAI + D-UNL. S.A.G., M.G.R., and C.D.B. are members of CONICET, Argentina.

References

1. Zumft W (1997) Microbiol Mol Biol Rev 61:533–616
2. Richardson DJ, Watmough NJ (1999) Curr Opin Chem Biol 3:207–219
3. González PJ, Correia C, Moura I, Brondino CD, Moura JJG (2006) J Inorg Biochem 100:1015–1023
4. Young JPW (1996) Plant Soil 186:45–52
5. Galloway JN, Townsend AR, Erisman JW, Bekunda M, Cai Z, Freney JR, Martinelli LA, Seitzinger SP, Sutton MA (2008) Science 320:889–892
6. Gruber N, Galloway JN (2008) Nature 451:293–296
7. Aneja VP, Schlesinger WH, Erisman JW (2008) Nat Geosci 1:409–411
8. Barnett MJ, Fisher RF, Jones T, Komp C, Abola AP, Barloy-Hubler F, Bowser L, Capela D, Galibert F, Gouzy J, Gurjal M, Hong A, Huizar L, Hyman RW, Kahn D, Kahn ML, Kalman S, Keating DH, Palm C, Peck MC, Surzycki R, Wells DH, Yeh KC, Davis RW, Federspiel NA, Long SR (2001) Proc Natl Acad Sci USA 98:9883–9888
9. Capela D, Barloy-Hubler F, Gouzy J, Bothe G, Ampe F, Batut J, Boistard P, Becker A, Boutry M, Cadieu E, Dréano S, Gloux S, Godrie T, Goffeau A, Kahn D, Kiss E, Lelaure V, Masuy D, Pohl T, Portetelle D, Pühler A, Purnelle B, Ramsperger U, Renard C, Thébault P, Vandenbol M, Weidner S, Galibert F (2001) Proc Natl Acad Sci USA 98:9877–9882
10. Finan TM, Weidner S, Wong K, Buhrmester J, Chain P, Vorhölter FJ, Hernandez-Lucas I, Becker A, Cowie A, Gouzy J, Golding B, Pühler A (2001) Proc Natl Acad Sci USA 98:9889–9894
11. Ferroni FM, Guerrero SA, Rizzi AC, Brondino CD (2012) J Inorg Biochem 114:8–14
12. Godden JW, Turley S, Teller DC, Adman ET, Liu MY, Payne WJ, LeGall J (1991) Science 253:438–442
13. Kukimoto M, Nishiyama M, Murphy MEP, Turley S, Adman ET, Horinouchi S, Beppu T (1994) Biochemistry 33:5246–5252
14. Inoue T, Gotowda M, Deligeer, Kataoka K, Yamaguchi K, Suzuki S, Watanabe H, Gohow M, Kai Y (1998) J Biochem 124:876–879
15. Suzuki S, Kohzuma T, Deligeer, Yamaguchi K, Nakamura N, Shidara S, Kobayashi K, Tagawa S (1994) J Am Chem Soc 116:11145–11146
16. Libby E, Averill BA (1992) Biochem Biophys Res Commun 187:1529–1535
17. Suzuki S, Kataoka K, Yamaguchi K, Inoue T, Kai Y (1999) Coord Chem Rev 190–192:245–265
18. Murphy LM, Dodd FE, Yousafzai FK, Eady RR, Hasnain SS (2002) J Mol Biol 315:859–871
19. Dennison C (2005) Coord Chem Rev 249:3025–3054
20. Inoue T, Nishio N, Suzuki S, Kataoka K, Kohzuma T, Kai Y (1999) J Biol Chem 274:17845–17852
21. Williams PA, Fulop V, Leung Y-C, Chan C, Moir JWB, Howlett G, Ferguson SJ, Radford SE, Hajdu J (1995) Nat Struct Mol Biol 2:975–982

22. Thompson GS, Radford SE, Leung Y-C, Redfield C, Ferguson SJ (2000) Protein Sci 9:846–858
23. Najmudin S, Pauleta SR, Moura I, Romao MJ (2010) Acta Crystallogr Sect F 66:627–635
24. Vakoufari E, Wilson KS, Petratos K (1994) FEBS Lett 347:203–206
25. Petratos K, Dauter Z, Wilson KS (1988) Acta Crystallogr Sect B 44:628–636
26. Impagliazzo A, Ubbink M (2004) J Am Chem Soc 126:5658–5659
27. Pauleta SR, Guerlesquin F, Goodhew CF, Devreese B, Van Beeumen J, Pereira AS, Moura I, Pettigrew GW (2004) Biochemistry 43:11214–11225
28. Torres MJ, Rubia MI, Bedmar EJ, Delgado MJ (2011) Biochem Soc Trans 39:1886–1889
29. Laming EM, McGrath AP, Guss JM, Kappler U, Maher MJ (2012) J Inorg Biochem 115:148–154
30. Low L, Kilmartin JR, Bernhardt PV, Kappler U (2011) Front Microbiol 2:58
31. Bradford MM (1976) Anal Biochem 72:248–254
32. Laemmli UK (1970) Nature 227:680–685
33. Stoll S, Schweiger A (2006) J Magn Reson 178:42–55
34. González PJ, Rivas MG, Brondino CD, Bursakov SA, Moura I, Moura JJG (2006) J Biol Inorg Chem 11:609–616
35. Correia C, Besson S, Brondino CD, González PJ, Fauque G, Lampreia J, Moura I, Moura JJG (2008) J Biol Inorg Chem 13:1321–1333
36. Pombeiro AJL, McCleverty JA (eds) (1993) Molecular electrochemistry of inorganic, bioinorganic, and organometallic compounds. Kluwer, Dordrecht
37. Lojou É, Bianco P (2000) J Electroanal Chem 485:71–80
38. Petratos K, Banner DW, Beppu T, Wilson KS, Tsernoglou D (1987) FEBS Lett 218:209–214
39. Solomon EI, Szilagyi RK, DeBeer George S, Basumallick L (2004) Chem Rev 104:419–458
40. Kukimoto M, Nishiyama M, Tanokura M, Adman ET, Horinouchi S (1996) J Biol Chem 271:13680–13683
41. Yamaguchi K, Shuta K, Suzuki S (2005) Biochem Biophys Res Commun 336:210–214
42. Hirst J (2006) Biochim Biophys Acta 1757:225–239
43. Paes De Sousa PM, Pauleta SR, Simões Gonçalves ML, Pettigrew GW, Moura I, Correia Dos Santos MM, Moura JJG (2007) J Biol Inorg Chem 12:691–698
44. Kakutani T, Watanabe H, Arima K, Beppu T (1981) J Biochem 89:463–472
45. Pinho D, Besson S, Brondino CD, de Castro B, Moura I (2004) Eur J Biochem 271:2361–2369
46. Veselov A, Olesen K, Sienkiewicz A, Shapleigh JP, Scholes CP (1998) Biochemistry 37:6095–6105
47. Olesen K, Veselov A, Zhao Y, Wang Y, Danner B, Scholes CP, Shapleigh JP (1998) Biochemistry 37:6086–6094
48. Prudêncio M, Eady RR, Sawers G (2001) Biochem J 353:259–266